ISBN: 978-3-95450-234-9 ISSN: 2673-5504 doi:10.18429/JACoW-SRF2023-WEPWB083

BASIC DESIGN AND CONSIDERATION OF LI-VAPOR CONTAMINATION FOR A-FNS SRF

T. Ebisawa†, QST, Rokkasho, Japan and KEK, Ibaraki, Japan
K. Hasegawa, A. Kasugai, M. Oyaizu, S. Sato, QST, Rokkasho, Japan
E. Kako, H. Sakai, K. Umemori, KEK, Ibaraki, Japan

Abstract

The Advanced Fusion Neutron Source (A-FNS) project is in progressing in Japan, QST Rokkasho institute. A-FNS will demonstrate a performance of the DEMO DT fusion reactor material. In order to perform the test, a high intensity deuteron beam accelerator will be used to produce a high flux neutron field which is similar to the 14 MeV DT neutron. The Superconducting Radio-Frequency linear accelerator (SRF) is one component of the A-FNS accelerator system. Although the A-FNS accelerator system design is based on the IFMIF design, the improvement of some subsystem has been considering by taking into account the lessons learnt from the LIPAc project. In order to keep a high stability and availability of the SRF performance, we plan to increase the number of SRF cavities and cryomodules considering the trouble or degradation of the cavity performance and modify the engineering design of some components. In addition, changing of the beam transport line design and Li vapor contamination study of SRF cavity are conducting. In this presentation, the progress of the SRF design and related activities for A-FNS in QST will be presented.

INTRODUCTION

The A-FNS project is in progressing at QST Rokkasho institute to conduct the fusion neutron irradiation tests of the materials for a fusion reactor by the accelerator driven neutron source system. The A-FNS accelerator will produce a Continuous Wave (CW) deuteron beam of 125 mA/40 MeV and inject to the Li target to generate neutrons with energy around 14 MeV which is similar to energy of the neutron generated by a DT fusion reactor [1].

As shown in Fig. 1, the A-FNS accelerator system consists of an injector system with ECR ion source and LEBT (Low Energy Beam Transport), Radio-Frequency Quadrupole accelerator (RFQ), Medium Energy Beam Transport (MEBT), multiple Superconducting Radio-Frequency linear accelerator (SRF linac) cryomodules (CM), High Energy Beam Transport (HEBT) and Beam Dump (BD). Table 1 shows the main specification of the A-FNS accelerator. The design is based on the International Fusion Materials Irradiation Facility (IFMIF) accelerator design [2]. In order to solve the concerns of the design and improve it, some components are to be improved by reflecting the outcomes of Linear IFMIF Prototype accelerator (LIPAc) commissioning and design of the IFMIF/EVEDA (Engineering Validation and Engineering Design Activities) project [2].

There is the inadequate energy margin design of the SRF linac as the concern. In order to keep a stable operation for 40 MeV, we redesigned the SRF linac lattice design. In addition, we reviewed some SRF components with considering the mechanical issues in LIPAc SRF activity and design.

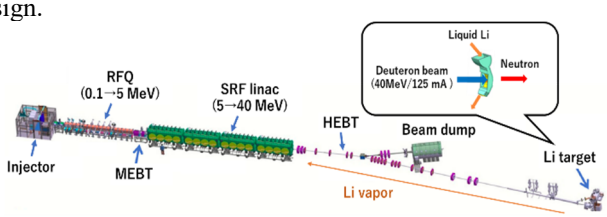

Figure 1: The schematic of the initial design of the A-FNS accelerator.

Table 1: Main Specification of the A-FNS Accelerator

Parameter	Value
Beam current	125 mA
Beam energy	40 MeV
Duty	CW
Beam profile at Li target	20 cm x 5 cm

There is the beam loss of the low energy particles which are not accelerated in the RFQ as another concern. From the results by beam dynamics simulation, the beam loss is too high so that thermal load is severe for the cooling system. To prevent the quench due to the thermal load, the energy filtering system is necessary to be installed in MEBT.

There is the unique issue of the A-FNS SRF which is the Li vapor contamination of the SRF cavity from the free surface liquid Li target. In order to minimize the Li vapor contamination, a concept of the dogleg HEBT has been introduced and its design is ongoing. Also, there are no information that the relation between the performance of the SRF cavity and the Li vapor contaminations. Therefore, we have investigated it to feedback for the design of the A-FNS accelerator system. For this study, we considered the Li vapor source apparatus to control the production of the nano scale mass vapor. The testing cavity for Li contamination study was prepared.

In this paper, the progress of the basic design of the A-FNS accelerator and the Li vapor contamination study are presented.

† ebisawa.takashi@qst.go.jp

ISBN: 978-3-95450-234-9 ISSN: 2673-5504 doi:10.18429/JACoW-SRF2023-WEPWB083

BASIC DESIGN OF THE A-FNS ACCELERATOR

Although the design of the A-FNS is based on the IFMIF accelerator system, some necessities of the improvements have been found by progressing the LIPAc project and reviewing the IFMIF design.

Regarding the injector and RFQ, there may be no major design change because the beam operation of the 125 mA/5 MeV at low duty cycle was succeed [3]. On the other hand, some improvements of the accelerator system design of the SRF, MEBT and HEBT should be considered.

Regarding the SRF linac, the main specification of the linac is same of the IFMIF design as shown in Table 2. The SRF linac will consist of the two types relativistic β Hale-Wave Resonator (HWR) cavities working 175 MHz at 4.45 K for accelerating the beam and the superconducting solenoid coils for focusing the beam [4].

Table 2: Main Specification of the A-FNS SRF

Parameter	Value
Frequency	175 MHz
Relativistic β (Low/High)	~0.1/~0.16
Temperature	4.45 K
Accelerating field	4.5 MV/m
Maximum solenoid field	6.0 T

IFMIF SRF linac does not have the enough margin of the beam acceleration energy when some troubles and degradations by field emission are occurred in cavity.

Reviewing the report of the SRF operation over the world, there are many troubles which cannot operate the SRF cavities and cause the degradation of the performance [5-7]. By referring these reports, we design the redundant SRF linac with 5 MeV to 6 MeV margin to do the stable 40 MeV beam operation in A-FNS as shown in Fig. 2. The maximum energy gain in SRF linac is about 40 MeV with 0.5 MeV/ low β HWRs x 26 and 1 MeV/ high β HWRs x 27. In addition, we increased the number of solenoid coils to focus the beam easier for preventing the beam loss with refereeing the DONES SRF linac design [8, 9].

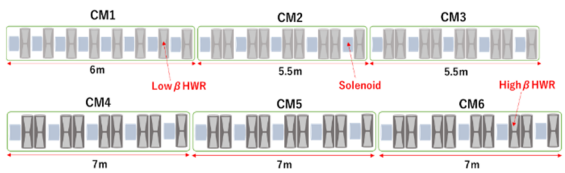

Figure 2: Improved SRF linac design for the A-FNS.

Figure 3 shows the result of the particle density distribution for the x and y direction by the beam dynamics simulation of TraceWin [10] with 10^6 test particles. The magnetic field of the solenoids were tuned to focus within tolerance which is lower than 16 mm. The accelerating field and phase were tuned to gain about 0.5 MeV and 1.0 MeV in low and high β HWRs, respectively. As a result, this design can have the 6 MeV margin. Table 3 shows the comparison with between the specification of the IFMIF design and those of the A-FNS design. Although A-FNS SRF linac design can have the margin, the total length is longer than IFMIF design.

However, the degradation by handling the high intensity deuteron beam and trouble of the solenoid failure issues are currently concerned in LIPAc SRF operation. The final design of the A-FNS SRF will be concluded by feedbacking the results based on the results by the LIPAc beam operation.

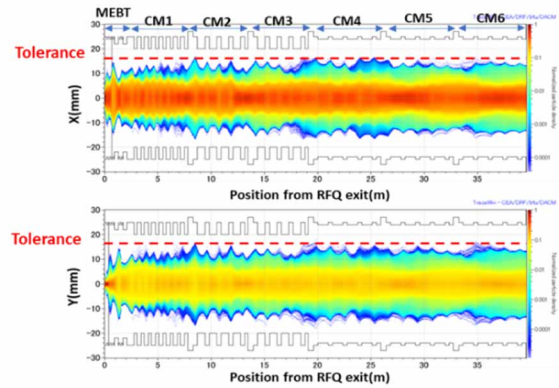

Figure 3: Result of the beam simulation for the A-FNS SRF.

Table 3: Comparison Between the IFMIF and A-FNS SRF

	IFMIF	A-FNS
Low β HWR	18	26
High β HWR	24	27
Solenoid	21	33
Beam energy	40MeV	46 MeV
Total length	~25 m	~38 m

Regarding the MEBT, the design of the energy filtering system for removing the low energy particle which is not accelerated in RFQ is considered to prevent beam loss in SRF linac. Figure 4 shows the result of comparing the beam loss simulation between with and without of the low energy particles. With low energy particles, the beam loss of about 5 to 10 W in SRF linac was estimated with using conventional MEBT. This heat load cause not only radiation but also the too high heat load for the He refrigeration system. For the filtering system, the concepts of the dogleg or chicane type beam transport line design and the idea of Wien filter will be introduced. Finally, the type of filtering system will be selected with considering the beam transport, cost, operation policy and realistic possibility.

Although the initial design with the beam dynamics simulation was done for the HEBT, the detailed system design had not been conducted yet. The HEBT is used to guide the deuteron beam from SRF to Li target system and remove the Li vapor from the Li target system to prevent Li vapor contamination of the SRF cavities. IFMIF HEBT is designed bending 9º [11]. On the other

ISBN: 978-3-95450-234-9 ISSN: 2673-5504 doi:10.18429/JACoW-SRF2023-WEPWB083

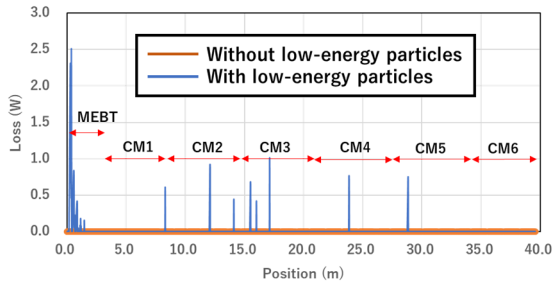

Figure 4: Comparison between the beam loss distribution of the with low energy particles from RFQ and that without ones.

hand, for A-FNS, the dogleg HEBT design will be introduced to reduce the back streaming of the Li vapor by 12 orders of magnitude compared with IFMIF design.

For keeping the performance of the SRF lianc, the basic design of the conceptual A-FNS accelerator system is symmetrized as shown in Fig. 5.

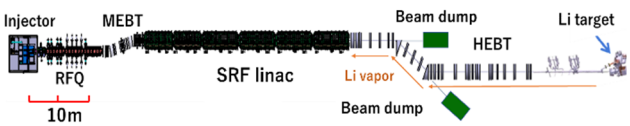

Figure 5: The schematic of the conceptual improved A-FNS accelerator.

DESIGN CHANGE OF THE SRF COMPONENTS

In the status of the LIPAc SRF, the assembly of the cryomodule is progressing [12]. Considering and reviewing the design or troubles, some design of the components will be changed.

For the LIPAc HWR cavities, the complete High-Pressure Rinsing (HPR) of the HWRs is difficult due to the interference of the nozzle to the accelerating gap [13]. To wash for all inner surface of the HWRs, the HPR port position will be changed by 45 degrees tilted position which is not to interfere the nozzle to accelerating gap. By simulation of the nozzle movement and water accessibility, it was conformed that the HPR can be completely done [14]. Figure 6 shows the comparing the LIPAc HWR design and improved HWRs.

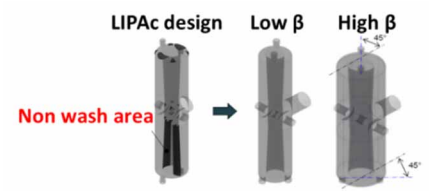

Figure 6: Changing and simulation of the HPR port. Black surface is non washing area.

Since the LIPAc cryostat was designed by the slide loading, the larger space was necessary to assemble the cryomodule. By referring the RIKEN cryomodule design, the top loading cryostat by covering design is considered for the A-FNS cryostat [15]. Figure 7 shows the LIPAc cryostat design and A-FNS design.

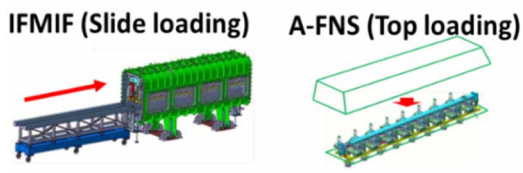

Figure 7: The schematic of cryostat design.

Regarding the superconducting solenoid coil, the major changes are considered. In fabrication of the solenoid tank with bellows by welding, there were many troubles of the vacuum leakage due to difficulties of the welding and processing. To prevent the troubles, bellows and tank will be separated and be assembled with screws. Figure 8 shows the schematic of the conceptual design of the separated solenoid coil.

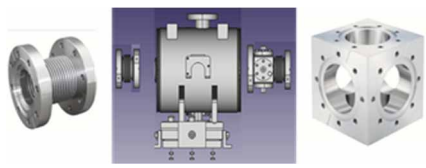

Figure 8: The schematic of the separated solenoid.

In addition, a screw and pins were dropped out in He tank that the human's hand and tool cannot access [12]. Concerning the unusable of the solenoid by breakage, quench and beam loss, the beam dynamics simulation was done to determine the optimum position and estimate the operation performance without some solenoids [16]. In conclusion, this cannot be major issues. However, it is unfavorable. In order to prevent the issue, solenoid structure was redesigned by introducing the split type of outer solenoid to access for fixing the inside of the solenoid. By using Superfich code, the conceptual split solenoid was designed. Figure 9 shows the result of the center magnetic field distribution for the split solenoid. Required magnetic field of 6 T can be applied with around 3 cm gap.

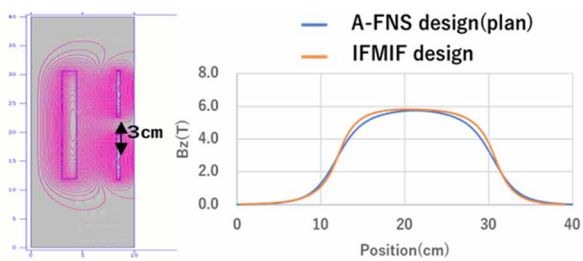

Figure 9: Calculation result of the split type solenoid.

LI VAPOR CONTAMINATION STUDY

As unique issue for the IFMIF and A-FNS, the Li vapor contamination from the Li target is considered. For designing the HEBT and investigating the relation between the SRF performance and the Li vapor, we have conducted the Li vapor contamination study of the SRF cavities by experimental study.

ISBN: 978-3-95450-234-9 ISSN: 2673-5504 doi:10.18429/JACoW-SRF2023-WEPWB083

From the results by the simple calculation, accumulated Li vapor at SRF exit is nano to about micro g/year. To control the small-scale vapor and set on vertical test (VT) system without vacuum breakage, Li vapor source apparatus with the alkali metal dispensers was designed. Figure 10 shows the picture of the Li vapor source apparatus and vacuum block diagram. To monitor the mass of Li vapor, the thin gauge was installed in the Li vapor flow line. As the test cavity to imitate the high field surface of the HWR, the 1.5 cell superconducting cavity which is used for electron gun was selected [17]. The 1.5 cell cavity in KEK was applied in the experiment.

After the assembly and leak test of the apparatus, the operation test was conducted. For the gaining the control range of the Li vapor, we investigated the relation between the current and evaporation rate. Figure 11 shows the result of the trend of the film thickness vs vacuum pressure, and Fig. 12 shows the result of the evaporation speed vs applying current for the Li dispenser. Initially, outgas was seen by low current as orange dots. Changing higher power supply and continuing the application of the current, the evaporation speed measured by the film thickness monitor was maximized 0.16 Å/ min in around 7.0 A as blue dots. This rate corresponds to the stacking 1 ng /hour and one layer for 10 min. From the results by this operation test, it was confirmed that controlling the nano scale-mass evaporation could be conducted. However, we cannot surely identify the Li atom. By a spectrum inspection and a residual gas measurement, there seemed not spectrum of Li or Li compound. The future task is to improve the apparatus for gaining more vapor and identify the Li.

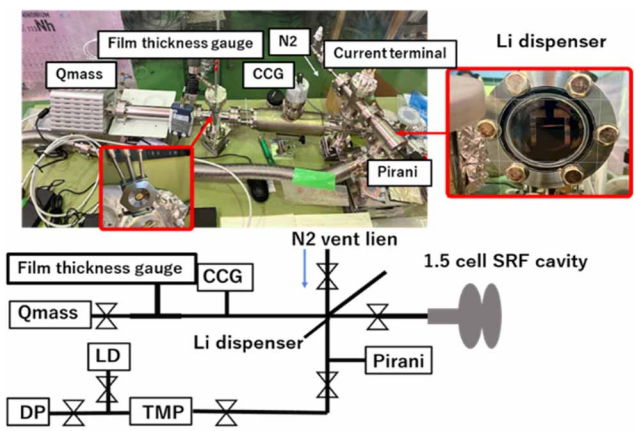

Figure 10: Assembled Li vapor source apparatus.

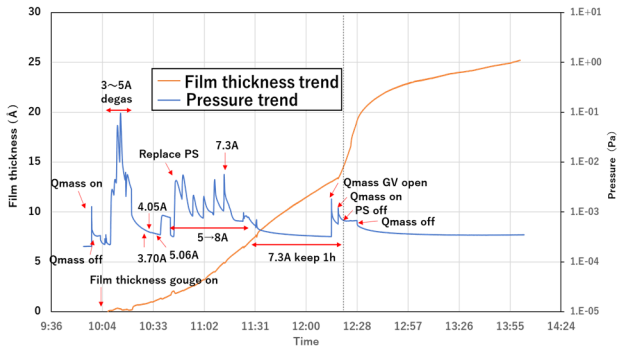

Figure 11: Result of the trend of the film thickness and the vacuum pressure.

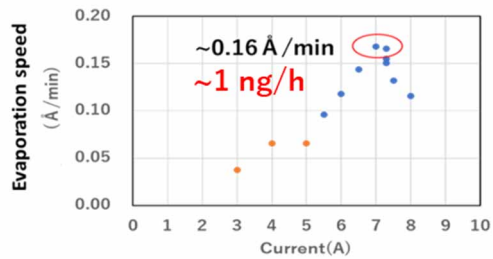

Figure 12: Result of the evaporation speed vs current. Orange dots is degassed by low power supply, blue dots is heat up by high power supply.

Regarding the test cavity, low power RF test for optimizing the length of the pickup and input antenna and the preparation in clean room were done. Figure 13 shows the picture of the 1.5 cell cavity and diagram of the low power test. Because of difficulty coupling the input and pick up with cavity, we used temporal antenna from choke side.

After the low power test, we conducted the HPR, assembled in cleanroom and tried VT for gaining the reference data without Li vapor as shown Fig. 14. In the current test, we cannot input the RF power by under coupling of the input antenna and some troubles are occurred during cooling down. We will conduct low power test with reviewing the experimental composition. After the second low power test, we are to conduct VT again later.

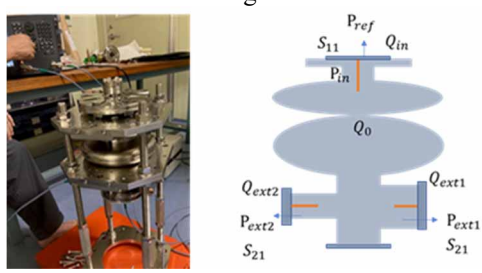

Figure 13: 1.5 cell cavity and schematic of the RF low power test.

ISBN: 978-3-95450-234-9 ISSN: 2673-5504 doi:10.18429/JACoW-SRF2023-WEPWB083

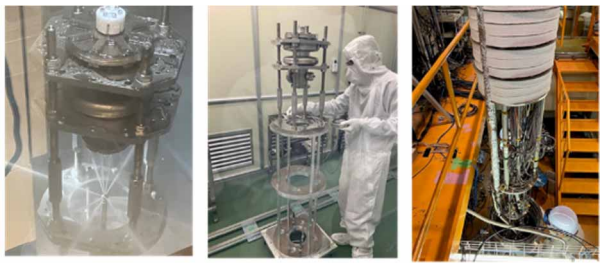

Figure 14: HPR assembly in clean room and set on VT system.

CONCLUSION

In this paper, the design and study for the A-FNS SRF related activity were introduced.

- Concept of the MEBT with energy filtering system to remove low energy particles from RFQ was introduced.
- SRF 6 CMs with 6 MeV energy margin was designed.
- Concept of the dogleg design of the HEBT for preventing Li vapor was introduced.
- Minor change of the SRF components that the HPR port of the HWRs, cryostat and solenoid were introduced.
- For the Li vapor contamination study, the Li vapor source was assembled and tested for controlling the nano scale vapor. We conducted low power test, HPR, assembled and VT of the 1.5 cell testing cavity. We will try VT again later.

In the future, we continue these activities for the realizing the A-FNS and fusion energy plant.

ACKNOWLEDGMENT

We wish to thank KEK for using the CST studio to analyses the SRF cavity and 1.5 cell cavity.

REFERENCES

[1] S. Sato *et al*., "Conceptual design of advanced fusion neutron source (A-FNS) and irradiation test modules", *Nucl. Fusion* vol. 61, no. 10, p. 106026, 2021. doi:10.1088/1741-4326/ac21f6

[2] J. Knaster *et al*., "IFMIF: overview of the validation activities", *Nucl. Fusion*, vol. 53, no. 11, p. 116001, 2013. doi:10.1088/0029-5515/53/11/116001

[3] K. Kondo *et al*., "Validation of the Linear IFMIF prototype accelerator (LIPAc) in Rokkasho", *Fusion Eng. Des.,* vol. 153, p. 11503, 2020.

[4] H. Dzitko *et al.*, "Technical and logistical challenges for IFMIF-LIPAc cryomodule construction", *Proc. SRF'15*, Whistler, BC, Canada, Sep. 2015, paper FRBA01, pp; 1453-1459.

[5] H. Sakai *et al.*, "Field emission studies in vertical test and during cryomodule operation using precise X-ray mapping system", *Phys. Rev. Accel. Beams,* vol. 22, no. 022022, pp. 1-22, 2019. doi:10.1103/PhysRevAccelBeams.22.022002

[6] Y. Yamamoto *et al.*, "Successful Beam Commissioning in STF-2 Cryomodules for ILC", presented at the 19th Int. Conf. on RF Superconductivity (SRF'19), Dresden, Germany, Jun.-Jul. 2019, paper WETEA6, unpublished.

[7] N. Sakamoto *et al*., "Commissioning of superconducting-linac booster for RIKEN heavy-ion linac", in *Proc. of 17th (PASJ'20)*, Sep. 2020, pp. 279-283. https://www.pasj.jp/web_publish/pasj2020/proceedings/PDF/FRPP/FRPP05.pdf

[8] N, Bazin *et al*., "Cryomodule development for materials irradiation facilities: from IFMIF/EVEDA TO IFMIF-DONES", in *Proc. of SRF'21*, East Lansing, MI, USA, Jun.-Jul. 2021, paper WEPFAV001, pp. 534-538. doi:10.18429/JACoW-SRF2021-WEPFAV001

[9] L. Du *et al*., "Beam dynamics studies for the IFMIF-DONES SRF-LINAC", in *Proc. of IPAC'18*, Vancouver, BC, Canada, 2018, paper TUPAF014, pp 987-690. doi:10.18429/JACoW-IPAC2018-TUPAF014

[10] D. Uriot and N. Pichoff, "Status of TraceWin Code", In *Proc. of IPAC'15*, Richmond, VA, USA, 2015, pp. 92-94. doi:10.18429/JACoW-IPAC2015-MOPWA008

[11] R. Duperrier, J. Payet, D. Uriot, "The IFMIF high energy beam transport line-errror studies", CEA Dapnia Lab., Paris, France, CEA Saclay DAPNIA-04-66 Rapport Interne.

[12] J. Chambrillon *et al.*, "Cleanroom assembly of the LIPAc cryomodule", presented at SRF'23, Grand Rapids, MI, USA, Jun. 2023, paper, this conference.

[13] G. Devanz *et al*., "Progress in IFMIF half wave resonators manufacturing and test preparation", in *Proc. SRF'15*, Whistler, Canada, Sep. 2015, paper THPB045, pp. 1191-1195.

[14] H. Hara *et al*., "High-pressure rinsing techniques of low-β superconducting RF cavity", in *Proc. of 18th (PASJ'21)*, Aug. 2021, paper WEP 036, pp. 702-705. https://www.pasj.jp/web_publish/pasj2021/proceedings/PDF/WEP0/WEP036.pdf

[15] K. Yamada *et al.*, "Construction of superconducting linac booster for heavy-ion linac at RIKEN Nishina Center", in *Proc. SRF'19*, Dresden, Germany, Jun.-Jul. 2019, pp. 502-507. doi:10.18429/JACoW-SRF2019-TUP037

[16] T. Ebisawa *et al.*, "Operational consideration in the LIPAc SRF with potential solenoid failure modes", presented at SRF'23, Grand Rapids, MI, USA, Jun. 2023, paper TUPTB031, this conference.

[17] T. Konomi *et al.*, "Development of high intensity, high brightness, CW SRF gun with bi-alkali photocathode", in *Proc. SRF'19*, Dresden, Germany, Jun.-Jul. 2019, pp. 1219-1222. doi:10.18429/JACoW-SRF2019-FRCAB4